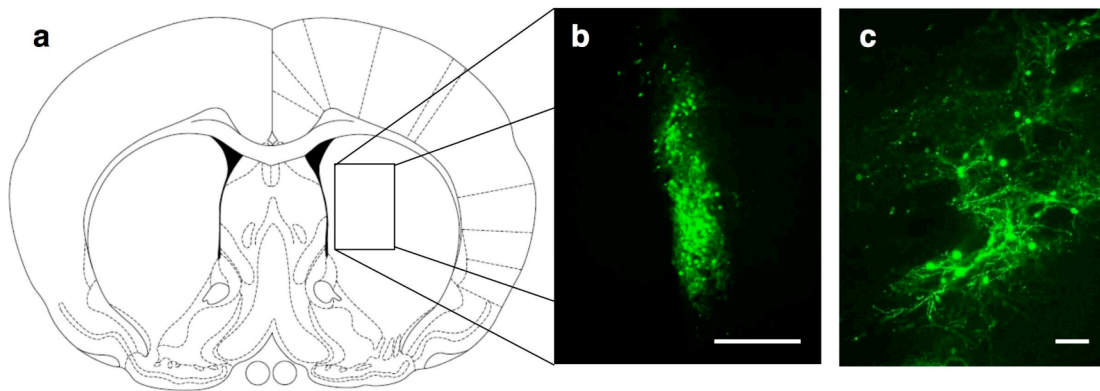
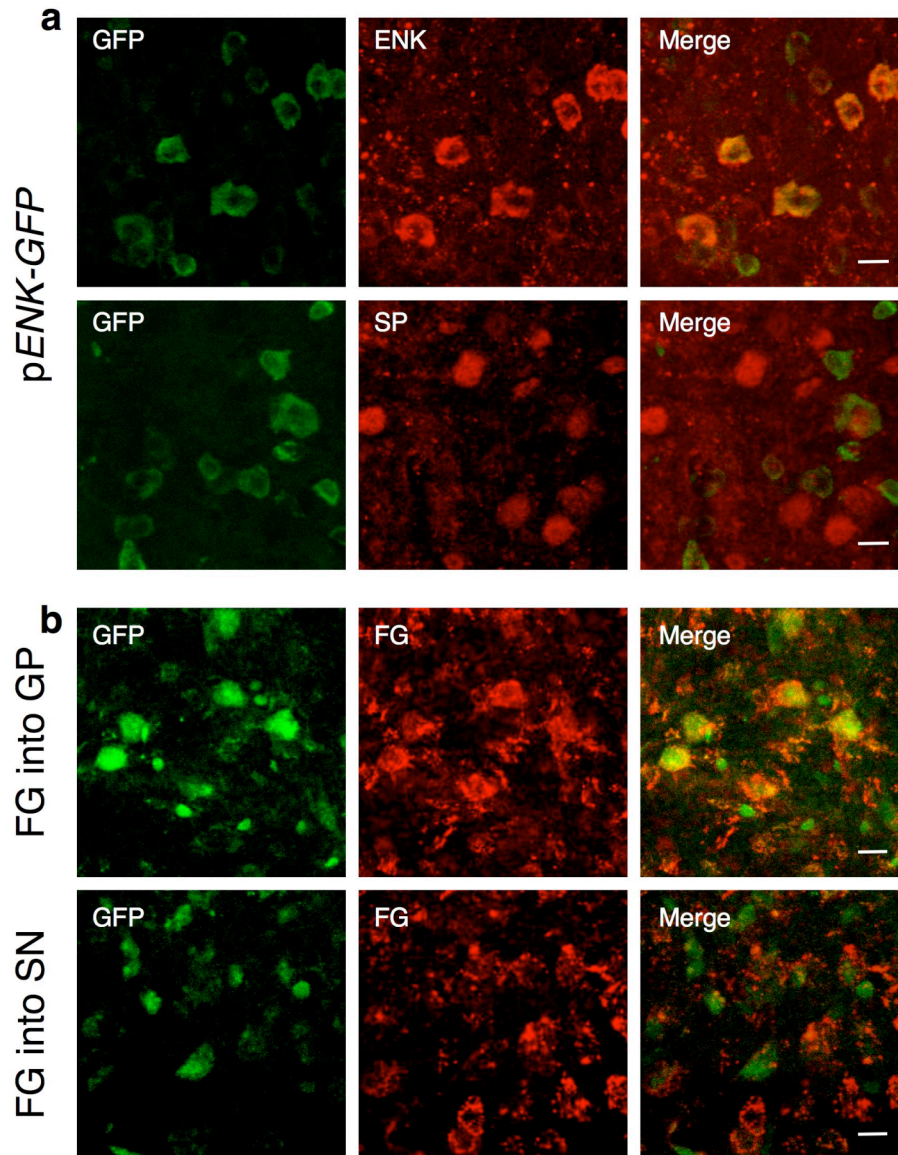


# Transient neuronal inhibition reveals opposing roles of indirect and direct pathways in sensitization

Ferguson SM, Eskenazi D, Ishikawa M, Wanat MJ, Phillips PEM, Dong Y, Roth BL and Neumaier JF

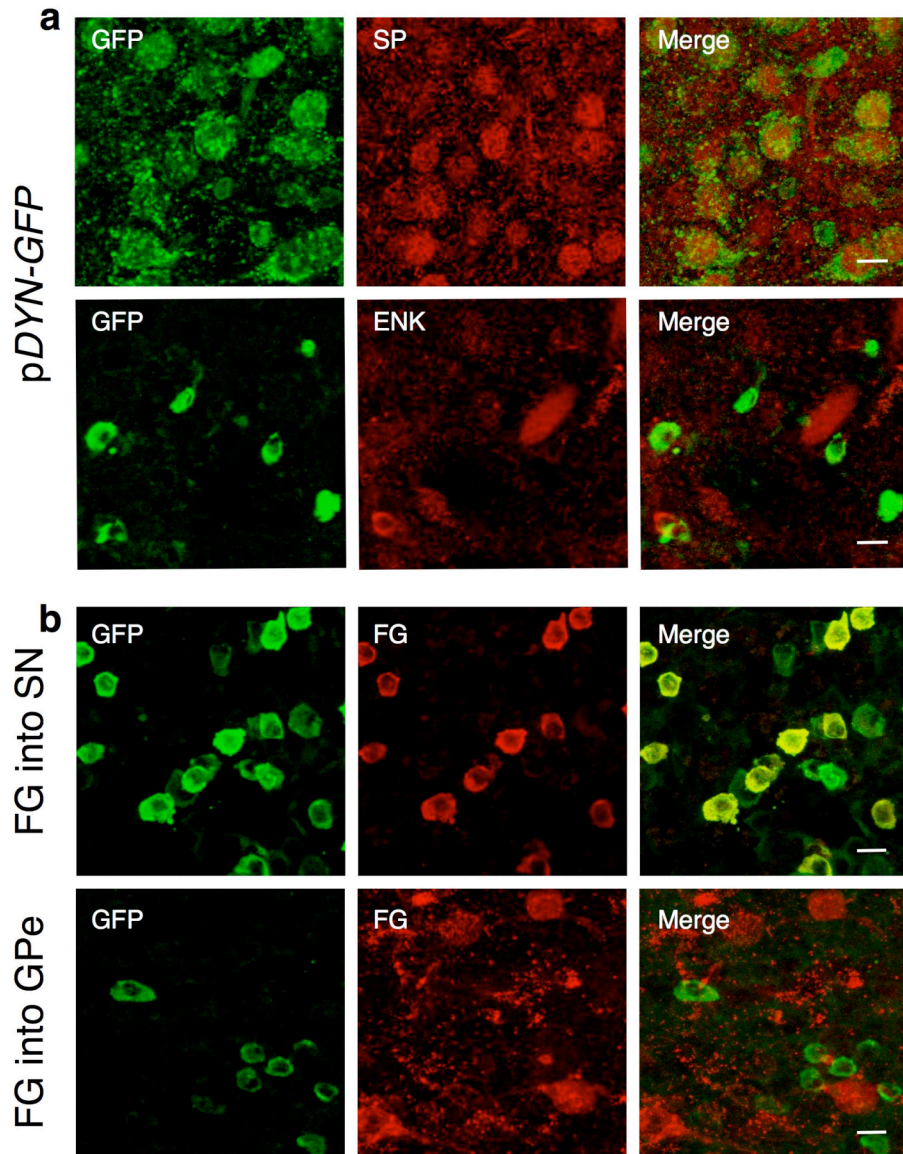


**Supplementary Figure 1** Representative depiction of viral spread. (a) Drawing adapted from plate 17 (0.2 mm from bregma) of the Paxinos and Watson rat atlas illustrating the region of viral spread on one coronal brain section. (b,c) Representative histological photomicrographs demonstrating GFP expression from a coronal section of the dorsomedial striatum following viral infusion. Scale bars, 1 mm (b) and 100  $\mu$ m (c).



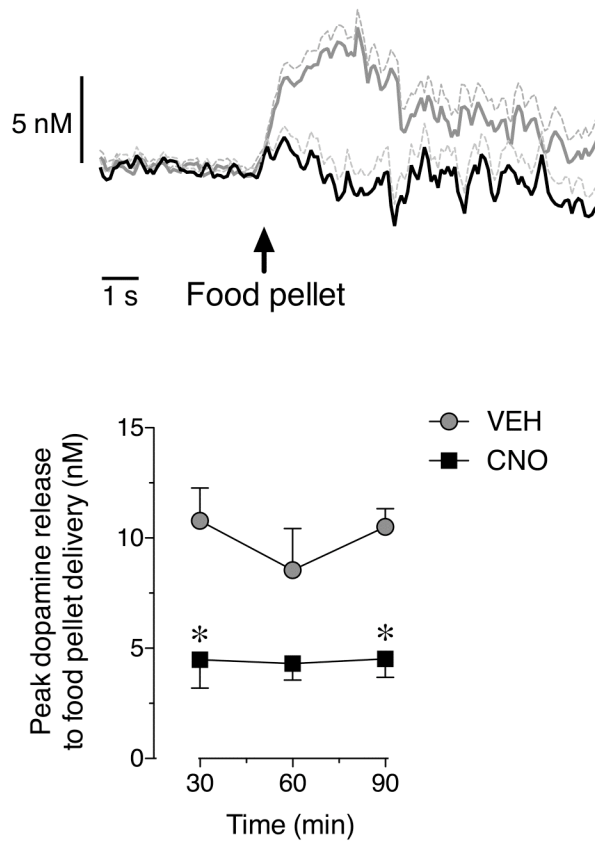
**Supplementary Figure 2** Expression of *pENK* viral vectors was restricted to striatopallidal neurons. **(a)** *pENK-GFP* was selectively expressed in striatopallidal MSNs (87% of GFP cells were ENK+, 150 out of 179; 4% of GFP cells were substance P+, 8 out of 195 cells). This is shown by co-localization (right, yellow) of GFP (left, green) and ENK+ striatopallidal MSNs (top middle, red) and absence of co-localization of GFP and substance P+ striatonigral MSNs (bottom middle, red). Scale bars, 10  $\mu$ m. **(b)** *pENK-GFP* was selectively expressed in indirect pathway neurons (90% of GFP cells were

Fluoro-Gold (FG)+ after GPe infusions, 111 out of 124 cells; 5% of GFP cells were FG+ after SNpr infusions, 3 out of 71 cells). This is shown by co-localization (right, yellow) of GFP (left, green) and striatal FG immunoreactivity (top middle, red) following infusions of FG into the GPe and absence of co-localization of GFP and striatal FG immunoreactivity (bottom middle, red) following infusions of FG into the SNpr. Scale bars, 10  $\mu$ m.

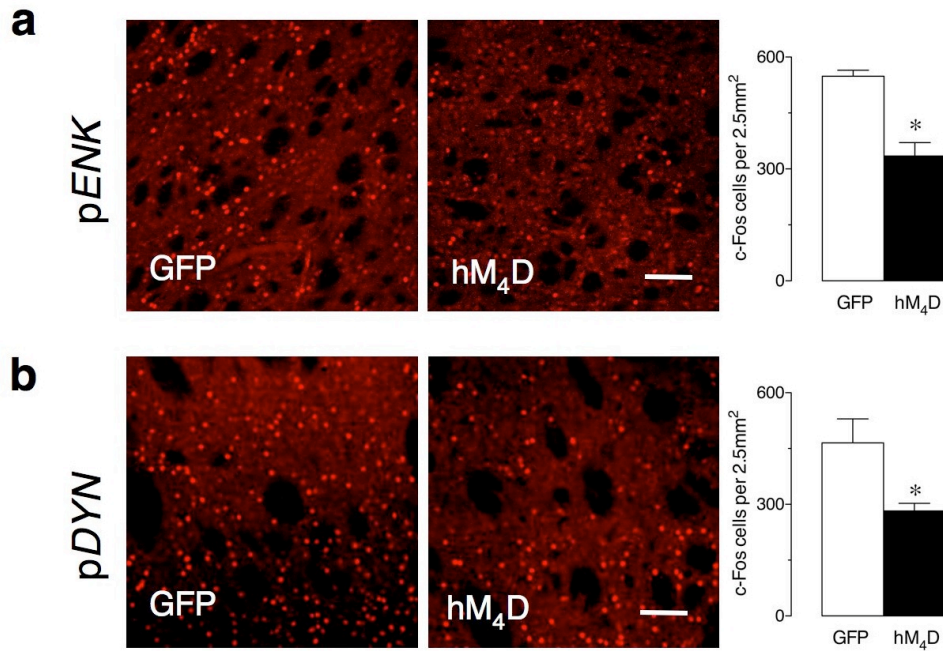


**Supplementary Figure 3** Expression of *pDYN* viral vectors was restricted to striatonigral neurons. (a) *pDYN-GFP* was selectively expressed in striatonigral MSNs (92% of GFP cells were substance P+, 232 out of 251 cells; 8% of GFP cells were ENK+, 10 out of 129 cells). This is shown by co-localization (right, yellow) of GFP (left, green) and substance P+ striatonigral MSNs (top middle, red) and absence of co-localization of GFP and ENK+ striatopallidal MSNs (bottom middle, red). Scale bars, 10  $\mu$ m. (b) *pDYN-GFP* was selectively expressed in direct pathway neurons (89% of GFP cells were FG+ after

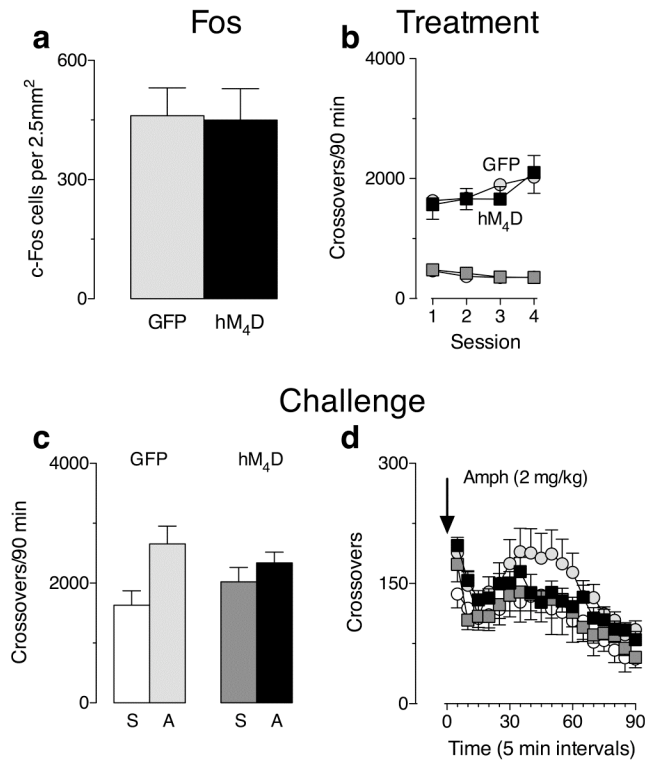
SNpr infusions, 157 out of 177 cells; 3% of GFP cells were FG+ after GPe infusions, 3 out of 90 cells). This is shown by co-localization (right, yellow) of GFP (left, green) and striatal FG immunoreactivity (top middle, red) following infusions of FG into the SNpr and absence of co-localization of GFP and striatal FG-immunoreactivity (bottom middle, red) following infusions of FG into the GPe. Scale bars, 10  $\mu$ m.



**Supplementary Figure 4** Activation of hM<sub>4</sub>D receptors in the VTA altered dopamine neurotransmission. Activation of hM<sub>4</sub>D receptors in the VTA during food pellet delivery significantly attenuated dopamine release at 0-30 min and 60-90 min post-CNO administration (Main effect of Treatment:  $F_{1,12} = 16.3$ ,  $P < 0.01$ ,  $*P < 0.05$  paired t-test versus VEH-treated group, bottom). Data is averaged across 90 min following administration of vehicle (VEH) or CNO (n=4, top).

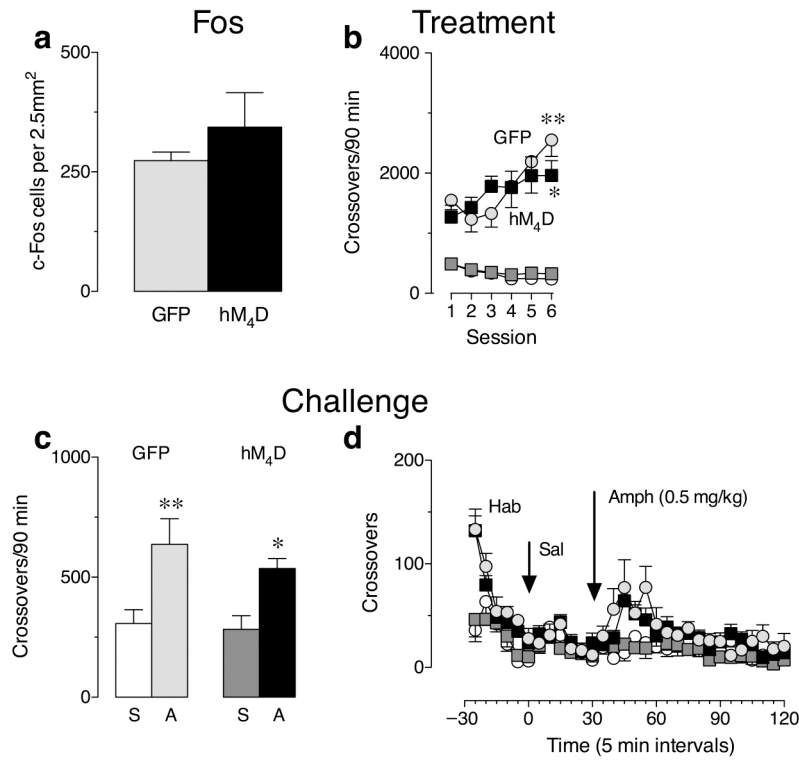


**Supplementary Figure 5** Activation of hM<sub>4</sub>D receptors in specific striatal cell populations reduced amphetamine-evoked c-Fos expression. CNO-mediated activation of pENK-hM<sub>4</sub>D (**a**) or pDYN-hM<sub>4</sub>D (**b**) receptors significantly decreased the number of amphetamine-induced Fos cells in dorsomedial striatum compared to control (GFP: pENK-GFP and pDYN-GFP, respectively) (pENK:  $t_6 = 5.41$ ,  $P = 0.002$ ,  $n=4$ /group; pDYN:  $t_9 = 2.48$ ,  $P = 0.04$ ,  $n=5-6$ /group). Data represent mean  $\pm$  SEM. Representative sections of Fos immunohistochemistry (red) are shown from GFP and pENK-hM<sub>4</sub>D (**a**) and pDYN-hM<sub>4</sub>D (**b**) infused striatum. Scale bars, 100  $\mu$ m.



**Supplementary Figure 6** Expression of pENK-hM<sub>4</sub>D receptors in the absence of CNO-mediated reduction of neuronal activity had no effect on biological responses to amphetamine. **(a)** Mere expression of pENK-hM<sub>4</sub>D receptors in the dorsomedial striatum had no effect on the number of amphetamine-evoked c-Fos cells ( $t_{10} = 0.10$ ,  $P = 0.92$ ,  $n=6/\text{group}$ ). **(b,c,d)** In the absence of activation, expression of pENK-hM<sub>4</sub>D receptors in the striatum had no effect on the development of amphetamine sensitization ( $n=8-10/\text{group}$ ). Treatment phase **(b)**: main effect of Session (S1 vs. S4:  $F_{1,17} = 5.19$ ,  $P = 0.04$ ; main effect of Virus:  $F_{1,17} = 0.0002$ ,  $P = 0.99$  and interaction between Virus and Session factors:  $F_{1,17} = 0.13$ ,  $P = 0.73$  not significant. Challenge phase **(c)**: main effect of Pretreatment:  $F_{1,32} = 4.23$ ,  $P = 0.048$ ; main effect of Virus:  $F_{1,32} = 0.13$ ,  $P = 0.72$  and interaction between Pretreatment and Virus factors:  $F_{1,32} = 0.70$ ,  $P = 0.41$  not significant.

Time course of the challenge response is shown in **(d)**. Thus, in the presence of CNO, *pENK-hM<sub>4</sub>D* receptor expression enhanced amphetamine sensitization compared to *pENK-GFP* (Figure 2), whereas, in the absence of CNO, *pENK-hM<sub>4</sub>D* receptor expression had no effect on sensitization to this threshold sensitization procedure. Data represent mean  $\pm$  SEM. S = saline, A = amphetamine. Squares represent hM<sub>4</sub>D groups, circles represent GFP groups. Light grey and black symbols represent rats that received amphetamine during the treatment phase, white and dark grey symbols represent rats that received saline during the treatment phase.



**Supplementary Figure 7** Expression of pDYN-hM<sub>4</sub>D receptors in the absence of CNO-mediated reduction of neuronal activity had no effect on biological responses to amphetamine. **(a)** Mere expression of pDYN-hM<sub>4</sub>D receptors in the dorsomedial striatum had no effect on the number of amphetamine-evoked c-Fos cells ( $t_9 = 1.03$ ,  $P = 0.33$ ,  $n=5-6/\text{group}$ ). **(b,c,d)** Expression without activation of pDYN-hM<sub>4</sub>D receptors in the striatum had no effect on the development of amphetamine sensitization ( $n=6/\text{group}$ ). Treatment phase **(b)**: main effect of Session (S1 vs. S6):  $F_{1,10} = 22.95$ ,  $P = 0.0007$ ; main effect of Virus:  $F_{1,1} = 2.75$ ,  $P = 0.13$  and interaction between Virus and Session factors:  $F_{1,10} = 0.75$ ,  $P = 0.41$  not significant,  $**P < 0.01$  and  $*P < 0.05$  versus Session 1. Challenge phase **(c)**: main effect of Pretreatment:  $F_{1,20} = 17.35$ ,  $P = 0.0005$ ; main effect of Virus:  $F_{1,20} = 0.80$ ,  $P = 0.38$  and interaction between Pretreatment and Virus factors:  $F_{1,20} = 0.30$ ,  $P = 0.59$  not significant,  $**P < 0.01$  and  $*P < 0.05$  versus saline-pretreated

group. Time course of the challenge response is shown in **(d)**. Thus, *pDYN-hM<sub>4</sub>D* receptor activation prevented the persistence of amphetamine sensitization (Figure 2), whereas in the absence of CNO, *pDYN-hM<sub>4</sub>D* receptor expression had no effect on the development of sensitization. Data represent mean  $\pm$  SEM. S = saline, A = amphetamine. Squares represent hM<sub>4</sub>D groups, circles represent GFP groups. Light grey and black symbols represent rats that received amphetamine during the treatment phase, white and dark grey symbols represent rats that received saline during the treatment phase.

## Supplemental Methods

**Subjects.** Male Sprague-Dawley rats (Harlan, Hollister, CA) weighing 250-274 grams upon arrival were housed two per cage and given a one-week acclimation period prior to any experimental manipulation. The housing room was temperature- and humidity-controlled and maintained on a 12:12 h light:dark cycle, with food and water available *ad libitum*.

**Drugs.** Amphetamine (Sigma, St. Louis, MO) was dissolved in sterile 0.9% saline and clozapine-*N*-oxide (BIOMOL Int., Plymouth Meeting, PA) was dissolved in sterile water. Drugs were administered by intraperitoneal (ip) injection in a volume of 1-2 ml/kg.

**Viral Vector Construction.** *pHSV-hM<sub>4</sub>D plasmid*. In order to construct a herpes simplex virus (HSV) vector that expresses a triple hemagglutinin epitope-tagged hM<sub>4</sub>D gene (1567 Kb), the hM<sub>4</sub>D gene was excised from a *pcDNA3.1* plasmid and inserted into a modified version of *pHSV-PrPUC* (kindly provided by Dr. Rachael Neve, McLean Hospital, Boston, MA). *pENK plasmids*. In order to construct an HSV vector that expresses green fluorescent protein (GFP) under the control of the enkephalin promoter, a ~2.7 Kb fragment (-2609 to +52) upstream of the enkephalin gene was excised from a *pREJCAT* plasmid (kindly provided by Dr. Sabol, NIH), subcloned into an intermediary *pGL3-basic* plasmid and inserted into a modified version of *pHSV-PrPUC*. In order to make an HSV vector that expresses the hM<sub>4</sub>D gene under the control of the enkephalin promoter, the hemagglutinin-tagged hM<sub>4</sub>D gene was excised from a *pcDNA3.1* plasmid and blunt-cloned into the *pENK-GFP* plasmid after removal of the GFP gene. *pDYN*

*plasmids*. To construct an HSV vector that expresses GFP under the control of the dynorphin promoter, a ~2.0 Kb fragment (-1858 to +135) upstream of the dynorphin gene was PCR cloned from rat genomic DNA using an upstream primer (5'-AAAGCTTAGGATAGAGATGAGAGAGGGCAGG-3') and a downstream primer (5'-GCTCTAGGTACCGATACTTACCTGCGTGCTGCTTTGTC-3') that also introduced a multiple-cloning site. The PCR product was sub-cloned into a TOPO plasmid using the Zero Blunt TOPO PCR cloning Kit (Invitrogen, Carlsbad, CA) and then inserted into the pHSV-PrPUC plasmid. To produce a version of this plasmid that expresses the hM<sub>4</sub>D gene, the hemagglutinin-tagged hM<sub>4</sub>D gene was excised from a pcDNA3.1 plasmid and blunt-cloned into the pDYN-GFP plasmid after removal of the GFP gene. For all plasmids, restriction mapping was used to identify successfully ligated clones and their entire sequences were confirmed by PCR. In order to prevent HSV promoter-driven "leakage" expression in non-targeted neurons, the promoter fragments and the GFP (or hM<sub>4</sub>D) genes were inserted in a reverse orientation with respect to the endogenous HSV promoter/origin of replication sequence, and two SV40 polyadenylation sequences were positioned between the end of the HSV promoter and the end of the GFP (or hM<sub>4</sub>D) genes. The amplicons were packaged into viral vectors using replication-deficient helper virus as described previously<sup>1</sup>.

**Surgery and viral gene transfer.** Rats were anesthetized with 2-4% isoflurane (Webster Veterinary Supply, Sterling, MA). Using standard stereotaxic procedures, 27-gauge stainless steel injectors were placed above targeted brain regions. Coordinates from bregma (mm) for dorsomedial striatum: A/P 0.2; M/L  $\pm$ 2.3; D/V -5.1 from skull surface,

for substantia nigra pars reticulata: A/P -5.3; M/L  $\pm$ 2.4; D/V -7.7 and for globus pallidus external: A/P -0.9; M/L  $\pm$ 2.7; D/V -6.2. Then, 3  $\mu$ l of either GFP (p*ENK* or p*DYN*, control) or hM<sub>4</sub>D (p*ENK* or p*DYN*) viral vector (~200,000 infectious units in 10% sucrose) was infused (unilaterally or bilaterally, depending on experiment) over a 15 min period at a flow rate of 0.2  $\mu$ l/min. The injector was left in place an additional 5 min to minimize diffusion up the injector tract. For tract tracing experiments, 2  $\mu$ l of either p*ENK-GFP* or p*DYN-GFP* viral vector was infused into the dorsomedial striatum and 1  $\mu$ l of a 2% Fluoro-Gold solution (Fluorochrome, Denver, CO) was infused into the SNpr or GPe. Experiments were carried out at 7-10 d post-infusion, based on pilot studies that examined the onset of gene expression. For electrophysiology experiments, 1  $\mu$ l of either p*HSV-GFP* or p*HSV-hM<sub>4</sub>D* was infused into the dorsal striatum. For voltammetry experiments, in-house constructed carbon-fiber electrodes were chronically implanted into the nucleus accumbens core (coordinates relative to bregma (mm): A/P 1.3; M/L  $\pm$ 1.3; D/V -7.0) for unilateral or bilateral voltammetric recordings and bilateral guide cannula were implanted above the ventral tegmental area (coordinates relative to bregma (mm): A/P -5.6; M/L  $\pm$ 0.5; D/V -7.0) for viral infusions. Starting 3 weeks post-surgery, rats were food restricted to ~90% of the free-feeding weight with an increase of 1.5% per week. To minimize neophobia, rats were pre-exposed to food pellets (45-mg food pellets, BioServ, NJ) in the home cage prior to magazine training in an operant chamber (Med Associates, VT). Once delivery of an unexpected food pellet delivery elicited a signal with a cyclic voltammogram that correlated ( $r^2 > 0.75$ ) with the template voltammogram of dopamine (see Fast-scan cyclic voltammetry section), rats received 2  $\mu$ l infusions of the neuron-specific p*HSV-hM<sub>4</sub>D* viral vector into the ventral tegmental

area through an infusion cannula that extended 1 mm past the guide cannula at a rate of 0.2  $\mu$ l/min. Experimental treatments were performed on days 3 and 4 post-virus infusion, corresponding to the time of maximal gene expression with this viral vector<sup>2</sup>. For all experiments, accuracy of injection coordinates was confirmed by visualization of GFP or hemagglutinin immunofluorescence or by cresyl violet staining of the injection needle tracts in 40  $\mu$ m tissue sections. Rats with injection sites outside of the targeted brain region were excluded from the experiments.

**Immunohistochemistry/Photomicrograph preparation.** Floating sections (40  $\mu$ m) were washed in 0.5% Triton-X/PBS for 10 min, then blocked in 5% normal goat serum (NGS)-0.25%Triton-X/PBS for 1 h. Sections were then incubated in 2.5% NGS-0.25%Triton-X/PBS containing antibodies to substance P (1:400, Chemicon/Millipore), GFP (1:400, Chemicon/Millipore), hemagglutinin (1:200, Chemicon/Millipore), Fluoro-Gold (1:8,000, Fluorochrome), and/or c-Fos (1:400, Santa Cruz) and/or in PBS containing methionine enkephalin (1:100, Immunostar) with gentle agitation at 4°C for 24 to 72 h. Next, sections were rinsed 4 times in PBS and incubated in species-appropriate Alexa 488 (green) and/or Alexa 568 (red)-conjugated goat secondary antibodies (1:500, Invitrogen, Carlsbad, CA) for 1 h. Sections were washed 2 times in PBS, mounted on slides and cover-slipped with Vectashield mounting medium with DAPI (Vectorlabs, Burlingame, CA). Images were captured with a Bio-Rad Radiance 2000 confocal system and an associated Nikon fluorescence microscope using an argon/krypton laser and red laser diode. For photomicrographs without immunohistochemistry, tissue sections were mounted on slides and cover-slipped with Vectashield mounting medium. Slides were

visualized with a Nikon Eclipse E600 with HyQ FITC, HyQ TRITC, and DAPI epifluorescence filters.

**Electrophysiology.** Two days following viral infusions of HSV viral vectors into the dorsal striatum, rats were decapitated following isoflurane anesthesia. Brains were removed, glued to a block and sliced with a vibratome in 4°C modified artificial cerebrospinal fluid (aCSF). Similar to previously described<sup>3</sup>, coronal striatal slices (300  $\mu$ m) were cut such that the preparation contained the signature anatomical landmarks (e.g. the anterior commissure) that delineated striatal subregions. After a 1-2 h recovery period, slices were transferred to a holding chamber to a submerged recording chamber where they were continuously perfused with oxygenated aCSF maintained at 33°C. Standard whole-cell recordings were made from the infected cells (identified by their GFP signals) and the uninfected cells (controls) using a MultiClamp 700B amplifier (Molecular Device) through an electrode (2-6 M $\Omega$ ) in all electrophysiological experiments<sup>3,4,5,6</sup>. The slices were continuously perfused with regular oxygenated aCSF (in mM: 119 NaCl, 2.5 KCl, 1.0 NaH<sub>2</sub>PO<sub>4</sub>, 1.3 MgCl<sub>2</sub>, 2.5 CaCl<sub>2</sub>, 26.2 NaHCO<sub>3</sub>, and 11 glucose, 290–295 mOsm, equilibrated at 31–34°C with 95% O<sub>2</sub>/5% CO<sub>2</sub>). Current-clamp recordings were used to measure evoked action potential firing, in which the resting membrane potential was adjusted to -80 mV. Input resistance was measured as the potential changes upon injected currents between – 150 pA and 150 pA). For these experiments, a K<sup>+</sup>-based internal solution was used (in mM: 130 K-methanesulfate, 10 KCl, 10 HEPES, 0.4 EGTA, 2.0 MgCl<sub>2</sub>, 3.0 MgATP, 0.5 Na<sub>3</sub>GTP, pH 7.2–7.4; 290–300 mOsm). Electrophysiological recordings were made from MSNs located in the striatum.

The MSNs, which comprise >90% of all neuronal types in the striatum, could be readily identified in the experimental condition by their mid-sized somas as well as their electrophysiological characteristics, such as hyperpolarized resting membrane potentials, long latency before the first action potential, lack of the  $I_h$  component, and rectification of the I-V curve at hyperpolarized voltages<sup>7</sup>.

**Fast-scan cyclic voltammetry.** During all experimental sessions, the chronically implanted microelectrodes were connected to a head-mounted voltammetric amplifier, which interfaces with a PC-driven data acquisition system (National Instruments, TX) through an electrical swivel (Med Associates, VT) mounted above the operant chamber. The electrodes were held at -0.4 V against an Ag/AgCl reference. Scans every 100 ms consist of ramping up to +1.3 V and back to -0.4 V at 400 V/s in a triangular fashion. Waveform generation for voltage ramps, data acquisition and analysis was carried out on a PC-based system using software written in LabVIEW (National Instruments, TX). Data were five-point smoothed and the concentration of dopamine was calculated through chemometric analysis<sup>4</sup>. Rats received CNO (3 mg/kg) or vehicle (counterbalanced within subject design on days 3 and 4 post-virus infusion) 10 minutes prior to initiating data collection. A single food pellet was delivered on a variable interval schedule of 5 minutes over the next 90 minutes (18 pellets given).

**Locomotor sensitization.** For experiments using the pENK viral vectors, the locomotor activating effects of amphetamine were measured using locomotor activity boxes (22 x 45 x 23 cm; San Diego Instruments, San Diego, CA). Briefly, 7 days following viral

infusions rats received four injections of amphetamine (2 mg/kg) or vehicle over an 8-day treatment period (one injection ~ every other day). This protocol was designed to induce threshold amphetamine sensitization in GFP control rats. Thirty minutes prior to each drug treatment, rats received an injection of CNO (1 mg/kg) or vehicle and returned to their home cage. Rats then received injections of amphetamine or vehicle and were placed into the locomotor activity boxes. Following a one-week withdrawal period all rats received a 2 mg/kg amphetamine challenge in the absence of CNO pre-treatment. Behavior was recorded for 90 min during each test session. As an additional control, a similar experiment was performed in animals that received *pENK* viral infusions, except all animals received a vehicle pre-treatment during the treatment sessions (i.e., no animals received CNO injections during the experiment). The number of cage crossovers, defined as two consecutive beam breaks - photobeams spaced 2" apart, was used as an index of locomotor activity. For experiments using the *pDYN* viral vectors, rats received six injections of amphetamine (2 mg/kg) or vehicle over an 8-day treatment period (one injection ~ every day). This protocol produces consistent amphetamine sensitization in GFP control rats. Thirty minutes prior to each drug treatment, rats received an injection of CNO (1 mg/kg) or vehicle and returned to their home cage. Following a one-week withdrawal period all rats received a 30-min habituation period to the locomotor activity boxes, followed by an injection of saline (behavior recorded for 30 min) and a 0.5 mg/kg amphetamine challenge in the absence of CNO pre-treatment (behavior recorded for 90 min).

**Fos expression.** Ten days following viral infusions, rats were transported to a novel test environment and given an injection of vehicle or CNO (3 mg/kg) followed 30 minutes later by an injection of amphetamine (5 mg/kg). Two hours later, rats were perfused transcardially with phosphate-buffered saline (PBS) followed by 4% paraformaldehyde. Brains were post-fixed for 4 h in paraformaldehyde and transferred to PBS until processed for immunohistochemistry.

**Statistics.** Group differences in locomotor activity, electrophysiology, fast-scan cyclic voltammetry and the number of c-Fos<sup>+</sup> cells were tested using two-way analyses of variance (ANOVAs; with or without repeated measures as warranted) followed by Bonferroni's post-hoc tests with corrections or unpaired t-tests. For all comparisons,  $\alpha = 0.05$ . Statistical values for the Supplementary Figures are included in the figure legends. Statistical values from experiments in Figures 1 and 2 are included below.

Electrophysiology: Figure 1d,e; Data from d is expressed as a percent change from baseline in e. Paired t-test, \*  $P < 0.05$  hM<sub>4</sub>D before vs. hM<sub>4</sub>D after CNO application;  $P = 0.46$  control before vs. control after CNO application,  $n=4-5$ . Figure 1g;  $F_{3,85} = 11.08$ , two-factor ANOVA; \*\*  $P < 0.01$  hM<sub>4</sub>D vs. hM<sub>4</sub>D/CNO;  $P = 1.0$ , control vs. control/CNO). Expression of hM<sub>4</sub>D receptors alone did not alter input resistance ( $P = 0.84$ ) or action potential firing ( $P = 0.64$ ).

c-Fos: Figure 1k; t-test,  $t_9 = 4.197$ ,  $P = 0.002$ ,  $n=5-6$ /group; Figure 1n: t-test,  $t_9 = 2.29$ ,  $P < 0.05$ ,  $n=5-6$ /group). Figure 1l: t-test, hemagglutinin-positive,  $t_9 = 2.46$ ,  $P < 0.05$ ; hemagglutinin-negative,  $t_9 = 3.75$ ,  $P < 0.01$ ; Figure 1o: t-test, hemagglutinin-positive,  $t_9 = 2.36$ ,  $P < 0.05$ ; hemagglutinin-negative,  $t_9 = 1.82$ ,  $P = 0.1$ .

Acute amphetamine response: Figure 2a: 2 way ANOVA, main effect of Treatment:  $F_{1,34} = 71.67$ ,  $P < 0.0001$ ,  $n = 9-10/\text{group}$ ,  $***P < 0.001$  versus saline-treated groups; main effect of Virus:  $F_{1,34} = 1.82$ ,  $P = 0.19$  and interaction between Treatment and Virus factors:  $F_{1,34} = 2.58$ ,  $P = 0.12$  not significant. Figure 2e: 2 way ANOVA, main effect of Treatment:  $F_{1,32} = 85.62$ ,  $P < 0.0001$ ,  $n = 8-10$ ,  $***P < 0.001$  versus saline-treated groups; main effect of Virus:  $F_{1,32} = 0.49$ ,  $P = 0.49$  and interaction between Treatment and Virus factors:  $F_{1,32} = 0.19$ ,  $P = 0.67$  not significant.

Sensitization: Figure 2b; 2 way RM ANOVA, main effect of Virus:  $F_{1,18} = 10.61$ ,  $P = 0.004$ ; main effect of Session (S1 vs. S4):  $F_{1,18} = 27.68$ ,  $P < 0.0001$  and interaction between Virus and Session factors:  $F_{1,18} = 4.71$ ,  $P = 0.04$ ,  $***P < 0.001$  versus Session 1,  $###P < 0.001$  versus amphetamine-treated GFP group). Figure 2c,d; 2 way ANOVA, main effect of Virus:  $F_{1,34} = 8.09$ ,  $P = 0.008$ ; main effect of Pretreatment:  $F_{1,34} = 14.96$ ,  $P = 0.0005$  and interaction between Virus and Pretreatment factors:  $F_{1,34} = 4.22$ ,  $P = 0.047$ ,  $***P < 0.001$  versus saline-pretreated group,  $###P < 0.01$  versus amphetamine-pretreated GFP group). Figure 2f; 2 way RM ANOVA, main effect of Session (S1 vs. S6):  $F_{1,18} = 22.81$ ,  $P = 0.0002$ ; main effect of Virus:  $F_{1,18} = 1.11$ ,  $P = 0.31$  and interaction between Virus and Session factors:  $F_{1,18} = 0.68$ ,  $P = 0.42$  not significant,  $**P < 0.01$  and  $*P < 0.05$  versus Session 1. Figure 2g,h; 2 way ANOVA, main effect of Pretreatment:  $F_{1,32} = 12.97$ ,  $P = 0.001$  and interaction between Virus and Pretreatment factors:  $F_{1,32} = 7.56$ ,  $P = 0.01$ ; main effect of Virus:  $F_{1,32} = 0.87$ ,  $P = 0.36$  not significant;  $***P < 0.001$  versus saline-pretreated groups,  $\#P < 0.05$  versus amphetamine-pretreated GFP group.

1. Clark, M.S., Sexton, T.J., McClain, M., Root, D., Kohen, R., & Neumaier, J.F. *J Neurosci* **22**, 4550-4562 (2002).
2. Barot, S.K., Ferguson, S.M., & Neumaier, J.F. *Eur J Neurosci* **25**, 3125-3131 (2007).
3. Ishikawa, M., Mu, P., Moyer, J.T., Wolf, J.A., Quock, R.M., Davies, N.M., Hu, X.T., Schluter, O.M., & Dong, Y. *J Neurosci* **29**, 5820-5831 (2009).
4. Dong, Y., Cooper, D.C., Nasif, F., Hu, X., & White, F.J. *J Neurosci* **24**, 3077-3085 (2004).
5. Dong, Y., Green, T., Saal, D., Marie, H., Neve, R., Nestler, E.J., & Malenka, R.C. *Nat Neurosci* **9**, 475-477 (2006).
6. Huang, Y.H., Lin, Y., Brown, T.E., Han, M.H., Saal, D.B., Neve, R.L., Zukin, R.S., Sorg, B.A., Nestler, E.J., Malenka, R.C., & Dong, Y. *J Biol Chem* **283**, 2751-2760 (2008).
7. Wilson, C.J. & Groves, P.M. *J Comp Neurol* **194**, 599-615 (1980).
8. Heien, M.L., Khan, A.S., Ariansen, J.L., Cheer, J.F., Phillips, P.E., Wassum, K.M., & Wightman, R.M. *Proc Natl Acad Sci USA* **102**, 10023-10028 (2005).